Single-Channel Properties of a Rat Brain Endoplasmic Reticulum Anion Channel

A. G. Clark, D. Murray, and R. H. Ashley
Department of Biochemistry, University of Edinburgh, Edinburgh EH8 9XD, Scotland, United Kingdom

ABSTRACT Many intracellular membranes contain ion channels, although their physiological roles are often poorly understood. In this study we incorporated single anion channels colocalized with rat brain endoplasmic reticulum (ER) ryanodine-sensitive Ca^{2+}-release channels into planar lipid bilayers. The channels opened in bursts, with more activity at negative (cytoplasm-ER lumen) membrane potentials, and they occupied four open conductance levels with frequencies well described by the binomial equation. The probability of a protomer being open decreased from ~0.7 at −40 mV to ~0.2 at +40 mV, and the channels selected between different anions in the order $P_{SCN} > P_{NO_3} > P_{Br} > P_{Cl} > P_F$. They were also permeant to cations, including the large cation $Tris^+$ (P_{Tris}/P_{Cl} = 0.16). Their conductance saturated at 170 pS in choline Cl. The channels were inactivated by 15 μM 4,4′-diisothiocyanatostilbene-2,2′-disulfonic acid (DIDS) and blocked with low affinity (K_D of 1–100 μM) by anthracene-9-carboxylic acid, ethacrynic acid, frusemide (furosemide), HEPES, the indanyloxyacetic acid derivative IAA-94, 5-nitro-2-(3-phenylpropylamino)-benzoate (NPPB), and Zn^{2+}. Unlike protein translocation pores, the channels were unaffected by high salt concentrations or puromycin. They may regulate ER Ca^{2+} release, or be channel components en route to their final cellular destinations. Alternatively, they may contribute to the fusion machinery involved in intracellular membrane trafficking.

INTRODUCTION

Bilayer and patch-clamp recording studies have revealed non-ligand-gated surface membrane Cl^- channels in *Torpedo* electroplax (Miller, 1982), skeletal muscle sarcolemma (Blatz and Magleby, 1985), and the plasma membranes of epithelial (Landry et al., 1990) and neuronal (Blatz, 1991) cells. Many of these channels modulate membrane excitability or control cell volume by regulating water and electrolyte movements (Pusch and Jentsch, 1994). Anion channels are also present in intracellular membranes, including those of mitochondria (reviewed by Sorgato and Moran, 1993, and Colombini, 1994), the nucleus (Tabares et al., 1991; Rousseau et al., 1996), and the endoplasmic (Schmid et al., 1988; Ashley, 1989a,b; Simon and Blobel, 1991; Morier and Sauve, 1994) and sarcoplasmic (Smith et al., 1985, 1986; Tanifuji et al., 1987; Rousseau et al., 1988; Sukhareva et al., 1994; Townsend and Rosenberg, 1995; Kourie et al., 1996a,b) reticulum. For most of these intracellular channels, structural information is very sparse. Noteworthy exceptions include VDAC (the voltage-dependent anion-selective channel of mitochondria, see Colombini, 1994) and the putative bovine kidney Cl^- channel component p64 (Landry et al., 1992). p64 may be a member of an extensive channel protein family (Howell et al., 1996), but in this case there are few detailed single-channel data.

Sarcoplasmic reticulum (SR) Cl^- channels were used as a marker for membrane vesicle fusion in the planar bilayer experiments that led to the discovery of intracellular ryanodine-sensitive Ca^{2+} release channels in skeletal muscle (Smith et al., 1985). Similar experiments, using Cl^- channels to report the fusion of rat cerebral cortex microsomal membrane vesicles with bilayers (Ashley, 1989a,b), showed that ryanodine-sensitive Ca^{2+} channels are also present in brain microsomes (in endoplasmic reticulum membranes; Pozzan et al., 1994). Although single SR Cl^- channels have been studied in detail (Tanifuji et al., 1987; Rousseau et al., 1988; Townsend and Rosenberg, 1995; Kourie et al., 1996a,b), much less is known about brain endoplasmic reticulum (ER) anion channels, or the anion channels present in the ER of other tissues. In this report we describe a brain ER anion channel with a relatively wide pore (at least 7 Å in diameter). It shows marginal selectivity between different anions and is poorly selective for anions versus cations (which is not unusual for anion channels). Despite these features, its single-channel conductance is surprisingly low, saturating at 170 pS in choline Cl. We investigated the channel's "multimer"-type substate behavior, but it does not appear to have a "specific" pharmacological profile. The protomers are blocked with relatively low affinity (K_D (0 mV) = 135 μM) by the indanyloxyacetic acid derivative IAA-94, and by several other reagents. In common with many other Cl^- transporters, the channel is inactivated by 4,4′-diisothiocyanatostilbene-2,2′-disulfonic acid (DIDS). Despite their lack of specificity, these compounds may be useful tools for investigating the physiological role of the channel in ER vesicles and intact cells, where its function (like that of SR Cl^- channels) remains obscure.

Received for publication 17 October 1996 and in final form 12 April 1997.

Address reprint requests to Dr. R. H. Ashley, Department of Biochemistry, University of Edinburgh, George Square, Edinburgh EH8 9XD, Scotland, UK. Tel.: 44-31-650-3873; Fax: 44-31-650-3711; E-mail: richard.ashley@ed.ac.uk.

D. Murray's present address is Department of Bacteriology, Western Infirmary, University of Glasgow, Glasgow G11 6NT, Scotland, UK.

0006-3495/97/07/168/11 $2.00

MATERIALS AND METHODS

Membrane vesicles

Cerebral cortex microsomal membrane vesicles were isolated from adult male and female Sprague-Dawley rats as previously described (Ashley, 1989b; Martin and Ashley, 1993), in the presence of 0.2 μM (AEBSF), 10 μg/ml soybean trypsin inhibitor, 150 μg/ml benzamidine, 0.5 μg/ml leupeptin, 0.5 μg/ml pepstatin A, and 0.5 μg/ml aprotinin. Aliquots (10–20 mg protein/ml 0.32 M sucrose) were frozen in liquid N_2 and stored at −70°C for 1–3 months. These membranes bind ~0.5 pmol ryanodine/mg protein with a K_D of 5–10 nM (Ashley, 1989a,b), ~5% of the high-affinity ryanodine-binding capacity of skeletal muscle SR membrane vesicles (Lai et al., 1988). Brain membranes were also fractionated (Gray and Whittaker, 1962) to isolate mitochondria and synaptosomes. These were processed to obtain inner mitochondrial membrane vesicles (Chan et al., 1970) and synaptic plasma membrane vesicles (Cotman, 1974). Acid-precipitated membrane protein was measured by a standard Lowry procedure. All of these membrane vesicle fractions have been extensively characterized (e.g., Gray and Whittaker, 1962; Chan et al., 1970; Cotman, 1974).

Planar lipid bilayers

Planar bilayers were cast at room temperature by drawing ~0.5 μl of a decane suspension of palmitoyloleoyl phosphatidylethanolamine and palmitoyloleoyl phosphatidylserine (each 15 mg/ml; Avanti) across a 300-μm hole in a polystyrene partition separating two solution-filled chambers. Transmembrane currents through voltage-clamped bilayers (capacitance >250 pF, background conductance <5 pS) were low-pass filtered at 10 kHz (−3 dB cutoff, Bessel-type response) and recorded. Using standard voltage and current conventions, membrane potentials are quoted as cytoplasm minus ER lumen, and negative "outward" (cytoplasm to ER lumen) currents are shown as "downgoing" traces. The bilayers were initially bathed in 50–150 mM choline Cl containing 5 mM Tris-HCl (pH 7.4) and 2 mM $CaCl_2$. Membrane vesicles were added to the *cis* chamber to give 5–10 μg protein/ml, and a *cis* > *trans* osmotic gradient of at least 3:1 and constant stirring promoted vesicle-bilayer fusion. The contents of the *cis* chamber were changed by perfusion (10 volumes) to prevent further incorporation. Concentrated salt solutions, drugs, and other reagents were stirred into the relevant chamber (carrier solvents, e.g., dimethyl sulfoxide or ethanol, had no effect at the concentrations used). Experiments were terminated either by bilayer breakage or by irreversible channel inactivation (which occurred within ~30 min).

Analysis

We usually observed only one channel in the course of each experiment (~30 min), even during long periods where the probability of channels being open was very high (>0.7). Recording noise was 1.0–1.5 pA peak to peak at 0.25 kHz (−3 dB, low-pass 8-pole Besssel), rising to ~8 pA at 1 kHz. Single-channel currents (up to 5 pA) were postfiltered at 0.05–0.25 kHz (−3 dB, 8-pole Bessel or digital Gaussian filter) and analyzed using Axotape and pClamp software (Axon Instruments), with additional standard nonlinear fitting routines where appropriate. Channel amplitudes, and the proportion of time spent in substates, were measured by fitting multiple Gaussian distributions to amplitude histograms. For channel lifetime (closed time) analysis, where the nature and extent of low-pass filtering were critical, we adopted an iterative approach to determine the minimum cutoff frequency. Briefly, we set the filter's −3 dB point for each recording such that bilayer noise (in the absence of an incorporated channel) just failed to lead to the detection of false "openings" to the lowest-amplitude conductance level (determined after a preliminary amplitude analysis of a corresponding channel-containing recording). Under ideal conditions, the shortest directly measurable event durations should theoretically have had a rise time of $0.33/f_c$, where f_c is the −3 dB point in kHz (Colquhoun and Sigworth, 1983). That is, use of a cutoff frequency of 0.1 kHz should allow the duration of events as short as 3.3 ms to be measured. In practice, and as expected, we could not resolve the durations of events lasting less than ~4 or 5 ms when filtering at 0.1 kHz, even under quiet recording conditions. The filter cutoff frequency and the limits of our analysis are indicated in the Results section.

Relative ionic permeabilities (P) were calculated from appropriate forms of the Goldman-Hodgkin-Katz (GHK) voltage equation. Under biionic conditions, with monovalent anions X and Y in opposing chambers, P_X/P_Y was calculated from the reversal potential, E_r:

$$P_X/P_Y = [X]/[Y] \cdot \exp(-FE_r/RT)$$

R, T, and F have their usual meanings. In the presence of a single salt, relative anion versus cation permeabilities, P_{anion}/P_{cation}, were calculated from

$$P_{anion}/P_{cation} = [n - \exp(E_r/k)]/[n \cdot \exp(E_r/k)]$$

where n was the *cis:trans* salt concentration ratio, and $k = RT/F$. Where indicated, concentrations were corrected to give ionic activities. For the binomial analysis of channel gating, the probability of channel "protomers" (total number N) being open (P_o(protomer), or p) was calculated by fitting the data to a binomial model in which the proportion of time (P_i) spent in each state or conductance level, $i = 0, 1, \ldots, N$, was given by

$$P_i = \{N!\,[i!\,(N-i)!]\} \cdot p^i(1-p^i)^{N-i} \quad i = 0,1,\ldots,N$$

Data were fitted by maximizing the likelihood of $E(F_i)\ln(P_i)$, where F_i was the relative proportion of time in level i (Hayman and Ashley, 1993). For channels in which protomer openings conform to a binomial distribution, P_o(protomer) is given analytically by

$$P_o(\text{protomer}) = 1/N \cdot \sum_{n=1}^{N} P_i(n)$$

where $P_i(n)$ is the proportion of events at level n or higher, and n is at least the first substate (protomer) level. A similar calculation is available within the pClamp 6 suite of programs.

RESULTS

Brain ER contains ion channels with distinctive substate behavior

The anion channels described in this study are colocalized with brain ER ryanodine-sensitive Ca^{2+} release channels (Ashley, 1989a,b). Both channels often coincorporate in the same "fusion" event, and a Poisson analysis has supported the hypothesis that individual "fusion" events correspond to the incorporation of channel-containing "packets" with well-defined Ca^{2+} and Cl^- channel contents (Ashley, 1989b). We could also be confident about the orientation of the channels, because noninverted rather than inside-out ER vesicles fuse with bilayers (Ashley, 1989a,b; *cf.* skeletal muscle SR vesicles, Smith et al., 1985, 1986). The most compelling evidence for this orientation is that native ryanodine-sensitive Ca^{2+} channels almost invariably become incorporated with their binding sites for cytoplasmic ligands facing the *cis* chamber (as indicated, for example, by adenine nucleotide sensitivity). The *trans* chamber therefore corresponds to the ER lumen.

In choline Cl, coincorporated Ca^{2+} and K^+ channels were essentially silent (Smith et al., 1985, 1986; Tanifuji et al., 1987; Rousseau et al., 1988; Ashley, 1989a,b), and

anion channels were readily identified from Cl^- currents flowing *cis* to *trans* at 0 mV in fusion solutions. In KCl, coincorporated cation channels frequently gave rise to K^+ currents, and these recordings could not be clearly interpreted. Fig. 1 shows relatively long (40 s) recordings at negative (cytoplasm-lumen, Fig. 1 *A*) and positive (Fig. 1 *B*) holding potentials from a single anion channel in symmetrical 450 mM choline Cl. The voltage dependence of channel gating, with marked bursting behavior (especially at positive potentials), was typical. This asymmetry was present in every channel, consistent with a well-defined orientation for fusogenic vesicles. The channels exhibited distinctive substate behavior, with three substates at approximately 22%, 45%, and 71% of the main open level. During periods of activity at negative holding potentials, the channels tended to occupy relatively high-conductance substates or the fully open state (Fig. 1 *A*). At positive potentials the channels opened mainly to intermediate substates (Fig. 1 *B*). The substate behavior of the channel was a characteristic and consistent feature of all of the data in this study. In recordings lasting up to 30 min at a range of holding potentials, we never observed isolated "single-channel" currents equivalent in amplitude to a single substate, and every channel we examined exhibited the three identified subconductance levels (and no more than three). This behavior is illustrated in more detail in Fig. 2. The three substate levels adopted similar amplitudes relative to the main open state (defined as 100%, or fully open) in the chloride salts of choline, K^+, and $Tris^+$, irrespective of the particular cation (all of which were permeant; see below), and the mean substate amplitudes were 22 ± 2.1% (n = 16), 45 ± 4.4% (n = 22), and 71 ± 3.9% (n = 22), ± SD for n independent experiments. Similar values were obtained in CsCl (not shown).

We obtained anion channels with different conductance and gating behavior in about 1 in 20 experiments. We have no evidence that these were ER channels, and they were not studied further. Attempts to incorporate "ER-like" channels from brain mitoplast membrane vesicles (two preparations; see Materials and Methods) and brain synaptic plasma membrane vesicles (three preparations; see Materials and Methods) were unsuccessful.

Ionic conductance and selectivity

Fig. 3, *A–C*, shows a typical current/voltage (*I-V*) relationship for a single channel in symmetrical choline Cl with selected traces. The data are accompanied by a conductance/concentration relationship averaged from several experiments (Fig. 3 *D*). The main open-state slope conductance and the individual substate slope conductances were all linear (Fig. 3 *C*), with no evidence of rectification (at holding potentials up to ±60 mV) in any of the channels we examined. Recordings over a greater voltage range were limited by accelerated bilayer breakage, although control bilayers could be voltage-clamped at up to ±120 mV for periods of 0.5–1 min. This suggested that the incorporation of brain ER anion channels, or other components of the channel-containing vesicles, destabilized the membrane.

The relative permeabilities of a limited series of anions were measured by exposing channels to different K salts in the *cis* and *trans* chambers. Anion permeabilities relative to Cl^- were P_{SCN} (2.2 ± 0.8) > P_{NO_3} (1.4 ± 0.2) > P_{Br}

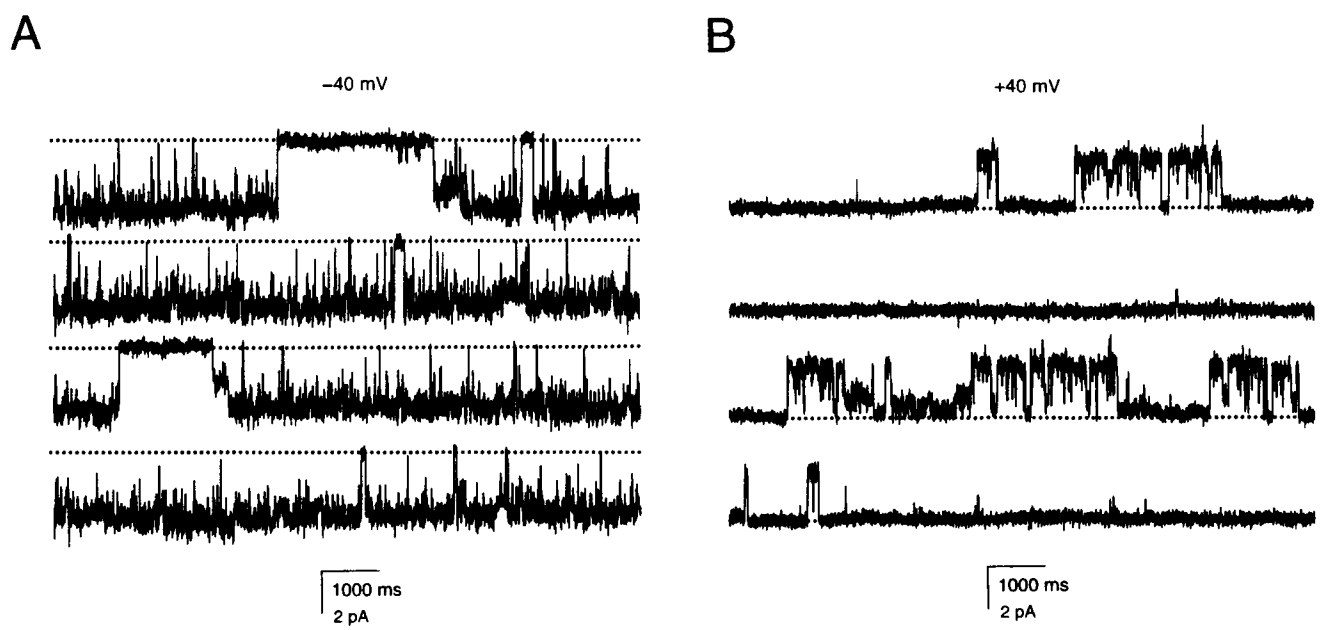

FIGURE 1 Ion channel recordings. Selected traces at −40 mV (*A*) and +40 mV (*B*) from a single channel in symmetrical 450 mM choline Cl. The potentials are *cis-trans* (equivalent to cytoplasm-ER lumen), and positive currents are shown as upgoing deflexions. The closed levels are indicated by dotted lines. Filtered at 0.15 kHz.

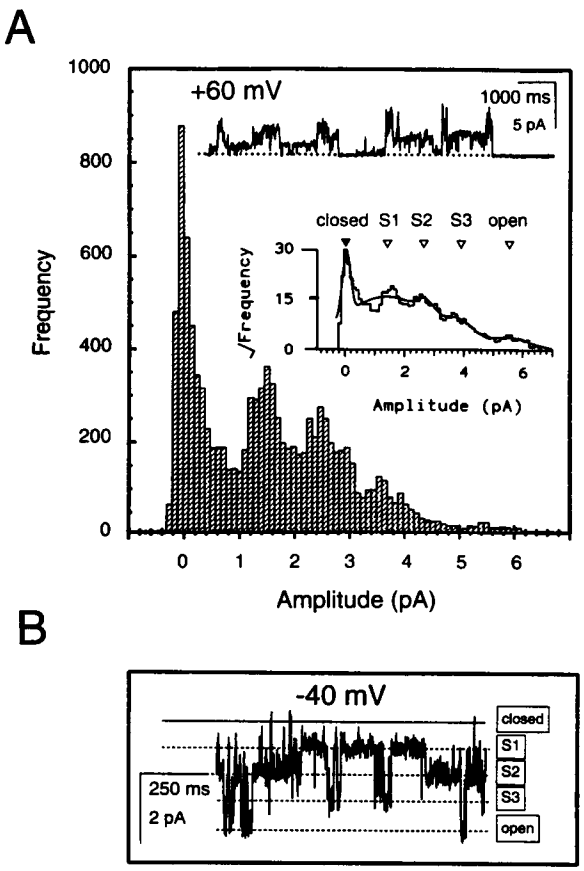

FIGURE 2 Substate behavior. (*A*) All-points amplitude histogram for a 10-s recording obtained in symmetrical 450 mM choline Cl (filtered at 0.05 kHz, closed level indicated). The inset square-root transformation (chosen to emphasize the small number of full openings) includes a least-squares fit to a multi-Gaussian distribution containing five components: closed, S1, S2, S3, and open, relative amplitudes 0/0.25/0.48/0.71/1.00. (*B*) Single-channel recording in 250 mM choline Cl, holding potential −40 mV (filtered at 0.15 kHz), showing the closed level (——) and all of the substates and the main open level (···). This trace was chosen to illustrate all of the substates in one short recording, and the gating pattern is not typical.

$(1.3 \pm 0.3) > P_{Cl} (= 1.0) > P_F (0.6)$, shown ± SD for three or four experiments, or averaged results from two determinations (all corrected for activities). The preference for the larger thiocyanate ion over Br^- and Cl^- is significant ($p < 0.05$). Anion versus cation permeabilities were examined in asymmetrical solutions of a given salt (Fig. 4), although relatively few data were obtained in KCl (and with other small cations) because we frequently uncovered K^+ (or other cation) currents flowing through previously silent, coincorporated cation channels. P_{anion}/P_{cation} was 1.6 ± 0.3 (mean ± SD, $n = 5$) for Cl^- versus K^+, 2.2 ± 0.2 ($n = 5$) for Cl^- versus choline$^+$, and 6.1 ± 0.2 ($n = 6$) for Cl^- versus $Tris^+$ (i.e., the preference of the channel for anions rather than cations increased as the size of the permeant cation was increased). The corresponding single-channel conductances were 74 ± 9 pS, 71 ± 3 pS, and 71 ± 13 pS, respectively. P_{Cl}/P_K was 1.7 ± 0.3 ($n = 5$) after correcting for ionic activities. Despite the permeability of $Tris^+$, mixtures of $Tris^+$ and $HEPES^-$ (125 mM Tris base neutralized with 250 mM HEPES free acid to a pH of 7.4) were impermeant (also see Smith et al., 1985, 1986; and Ashley, 1989a,b). Subsequent experiments indicated that $HEPES^-$ blocked the channel (described below). $P_{Cl}/P_{choline}$ was noted to be concentration-dependent, decreasing from 3.2 ± 1.2 ($n = 8$) in 250 mM versus 50 mM choline Cl to 2.2 ± 0.2 ($n = 5$) in 450 mM versus 150 mM ($p < 0.05$). Furthermore, P_{Cl}/P_{Cs} decreased from 4.3 ± 0.4 ($n = 3$) in 250 mM versus 50 mM to 2.4 ± 0.2 ($n = 3$) in 150 mM versus 50 mM CsCl (corrected for activities, $p < 0.001$).

Channel gating

The distinctive substate behavior of the channels suggested they had multibarreled pores. For example, a single polypeptide could have four conduction pathways, or four channels or channel subunits could be functionally coupled. The small differences in relative "protomer" conductances (0.22 and 0.23 for the first two protomers to open, then 0.26 and finally 0.29 for the third and fourth protomers) can be accommodated in this model if protomer conductance is sensitive to conformational changes associated with gating in neighboring protomers. Alternatively, membrane lipid might become incorporated in the pores. After a preliminary analysis of channel gating, a binomial analysis was used to test the hypothesis that channel gating corresponded to the operation of independent pores.

Intraburst closures were fitted by maximum-likelihood analysis to a double exponential distribution, leaving the small number of long-lived interburst closures unfitted (Fig. 5). We obtained evidence (not shown) for an additional closed time distribution with a mean lifetime of <5 ms, but most of these very brief events were poorly resolved (see Materials and Methods). Data collected over 30–120 s at −40 mV from six channels in symmetrical 250 mM choline Cl gave mean "short" closed times of 5.9 ± 1.6 ms and 47 ± 11 ms (means ± SD, $n = 6$). Analysis at +40 mV gave similar results, with mean "short" closed times of 7.7 ± 2.9 ms and 48 ± 12 ms ($n = 5$). Interburst closures were effectively excluded from the binomial analysis of a given channel by omitting closures more than threefold longer (i.e., 3 SD's greater) than the ~50 ms intraburst closed time constant. We also determined the minimum contiguous recording time required to obtain consistent results from a single channel (this was 30 s). The relative times spent in each substate (or open or closed) were measured by least-squares amplitude histogram analysis, as shown in Fig. 6, *A* and *B* (*smooth curves*).

P_o(protomer) at −40 mV and +40 mV was determined by maximum-likelihood analysis, and the values were used to construct the Gaussian distributions inset in Fig. 6, *A* and *B*. The striking similarity of calculated and measured distributions supported our interpretation of the gating of the channels at this level of resolution. Similar results were

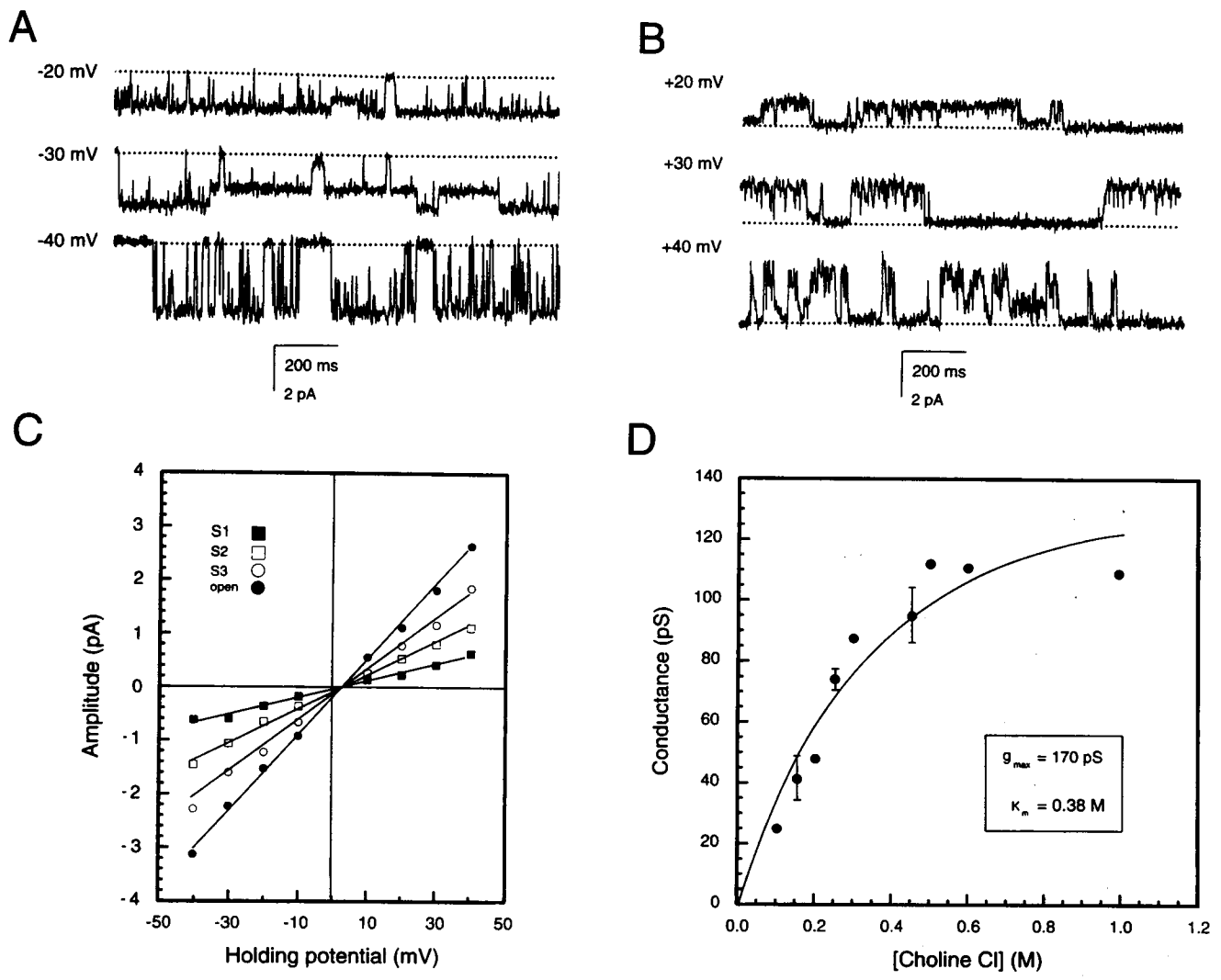

FIGURE 3 Conductance behavior in symmetrical choline Cl. (*A* and *B*) Selected traces in symmetrical 250 mM choline Cl, filtered at 0.1 kHz. Dotted lines indicate the closed current levels. In these traces the ~70% substate is prominent at −30 mV, and at +40 mV openings to the fully open state are almost completely absent. (*C*) Corresponding current/voltage (*I-V*) relationships for the main open state and the three substates. The slope conductance is 72 pS for the main open state, and there is a residual junction potential of +4 mV. (*D*) Single-channel conductance-concentration relationship in symmetrical choline Cl. All of the points are averages of at least two determinations, ± SEM (n = 4–12) where indicated. The data are fitted to a Michaelis-Menten model, $g = [S]/(K_m + [S]) \cdot g_{max}$, where g is the single-channel conductance, g_{max} is the maximum conductance, $[S]$ is the concentration of choline Cl, and K_m is the Michaelis constant.

obtained from limited recordings in KCl (not shown). The low frequency of some substate levels introduced the possibility of significant bias due to errors in measurement. Accordingly, if the overall residence time in a given level comprised <10% of the recording, the level was excluded from the fitting procedure. Results collected from six independent channels at a holding potential of −40 mV are summarized in Fig. 6 *C*. The correlation between the measured and predicted values for P_i was highly significant (slope = 0.97, $p < 0.001$), lending further support to the validity of a binomial analysis. The amplitude distributions at different potentials reflected a gradual decrease in the probability of protomers being open at increasingly positive potentials. In Fig. 6 *D*, the smooth curve is a least-squares fit to the Boltzmann equation

$$P_o(\text{protomer})/1 - P_o(\text{protomer}) = \exp[-zF/RT(V - V_0)]$$

where V is the membrane potential, V_0 is the potential where P_o(protomer) = 0.5 (this was −3.5 mV), and the small gating charge z is 0.84 (Fig. 6 *D*). When the curve was extrapolated, P_o(protomer) reached a maximum of 1.0 at −100 mV, and approached zero at +100 mV.

Channel modification and block

The channels remained active in the absence of added Ca^{2+}, and with 2 mM *cis* EGTA (pH 7.4, free $[Ca^{2+}] < 10$ nM).

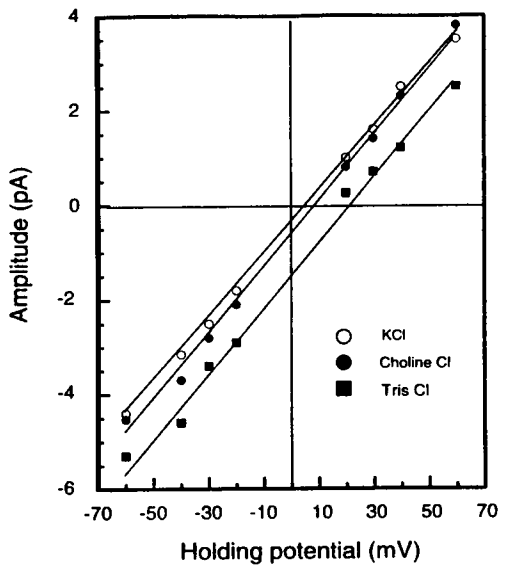

FIGURE 4 Relative cation permeabilities. Typical *I-V* relationships (for the fully open state) with 450 mM:150 mM KCl, choline Cl, or Tris Cl. Channel conductances are all ~65 pS, and reversal (equilibrium) potentials increase in the order Tris Cl > choline Cl > KCl. The Cl^- equilibrium potential in KCl, corrected for activities, is +25 mV.

Other reagents were stirred into the *cis* or *trans* chambers at the concentrations indicated in Table 1. Assuming that on binding the blocker the channel is rendered nonconducting, block was characterized as "slow" (or "intermediate") if individual blocking events could (nearly) be observed on the time scale of our recordings. Given that this will have required a residency time of at least 5 ms (see Materials and Methods), and assuming a forward rate constant limit of 10^8 $M^{-1} \cdot s^{-1}$, the K_D of such compounds must all be over 2 μM.

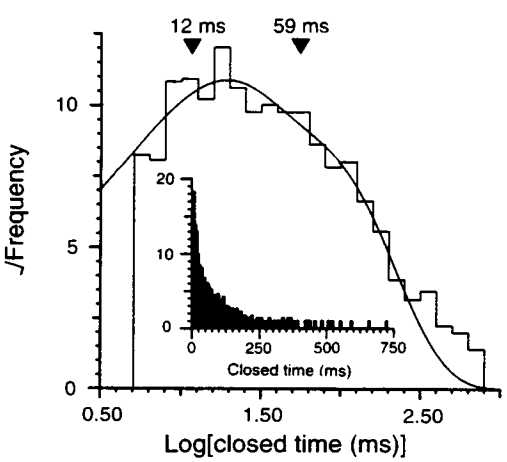

FIGURE 5 Closed lifetime analysis. Single-channel currents were recorded for 108 s at −40 mV in symmetrical 250 mM choline Cl, and the entire recording was subjected to lifetime analysis (filtered at 0.15 kHz). The closed and open levels were determined as described in the Materials and Methods and Results sections. Incompletely resolved events (<5 ms long) are excluded from the main histogram. The continuous line is the maximum-likelihood fit to a double-exponential pdf for closed durations between 5 ms and 250 ms. The two time constants are indicated. (*Inset*) Closed time distribution on a linear time scale.

Puromycin had no effect on channel activity, suggesting that the channels were not protein translocation pores (Simon and Blobel, 1991). The block induced by 9-AC (Palade and Barchi, 1977) and EA (Landry et al., 1987) was barely resolved or "intermediate," but HEPES blocked individual protomers (*cf.* Matsuda et al., 1989) for periods of up to hundreds of milliseconds (Fig. 7).

DIDS and the diuretic drug frusemide caused a complete, irreversible block and a "slow" block, respectively. The block induced by NPPB (Greger et al., 1987) increased with time of exposure, suggesting that the blocker may partition into the membrane to gain access to its binding site(s) (and NPPB was effective from either side of the membrane; Table 1). ATP (2 mM) (but not 2 mM Mg^{2+}) destabilized channel-containing membranes, interfering with experiments to uncover functional evidence for protein kinase A-mediated phosphorylation (Kawano et al., 1992). We do not know why this occurred, and in particular whether this resulted from an interaction with the channel or with other coincorporated vesicle components. Zn^{2+} blocked the channel from either side of the membrane, and block was essentially complete with a concentration of 2 mM.

The concentration- and voltage-dependence of IAA-94 block is illustrated in Fig. 8. Given that drug-binding rates (and often residency times) cannot be extracted from "multilevel" records, P_o(protomer) was measured to calculate the fractional occupancy of the putative blocker binding site as a function of blocker concentration [*B*], giving a K_D of 35 μM for the inhibitor at −30 mV (Fig. 8 *B*, *main panel*). Block was noted to be more marked at negative holding potentials, suggesting that the protomer blocker-binding sites were located within the membrane electric field. From the Woodhull equation:

$$*P_o(\text{protomer})/P_o(\text{protomer}) = *P_o/P_o$$

$$= \{1 + [B]/K_D(0) \cdot \exp(-z\delta FV/RT)\}^{-1}$$

where $*P_o$ and P_o are P_o(protomer) with (*) and without the blocker repectively, and $z\delta$, the "effective valence" of the blocking reaction, is the compound of valency and the electrical distance of the binding site. Assuming a valency of −1, δ was 0.78 of the distance across the membrane electric field when block was induced by 50 μM IAA-94 added to the *cis* chamber, and K_D(0 mV) was 135 μM.

DISCUSSION

A novel anion channel in brain ER

Intracellular Cl^- channels are well-recognized components of muscle SR (Smith et al., 1985, 1986; Tanifuji et al., 1987; Rousseau et al., 1988; Townsend and Rosenberg, 1995; Kourie et al., 1996a,b). In this study we reconstituted intermediate-conductance ER anion channels from rat brain. The channel discriminates poorly between different ions, dis-

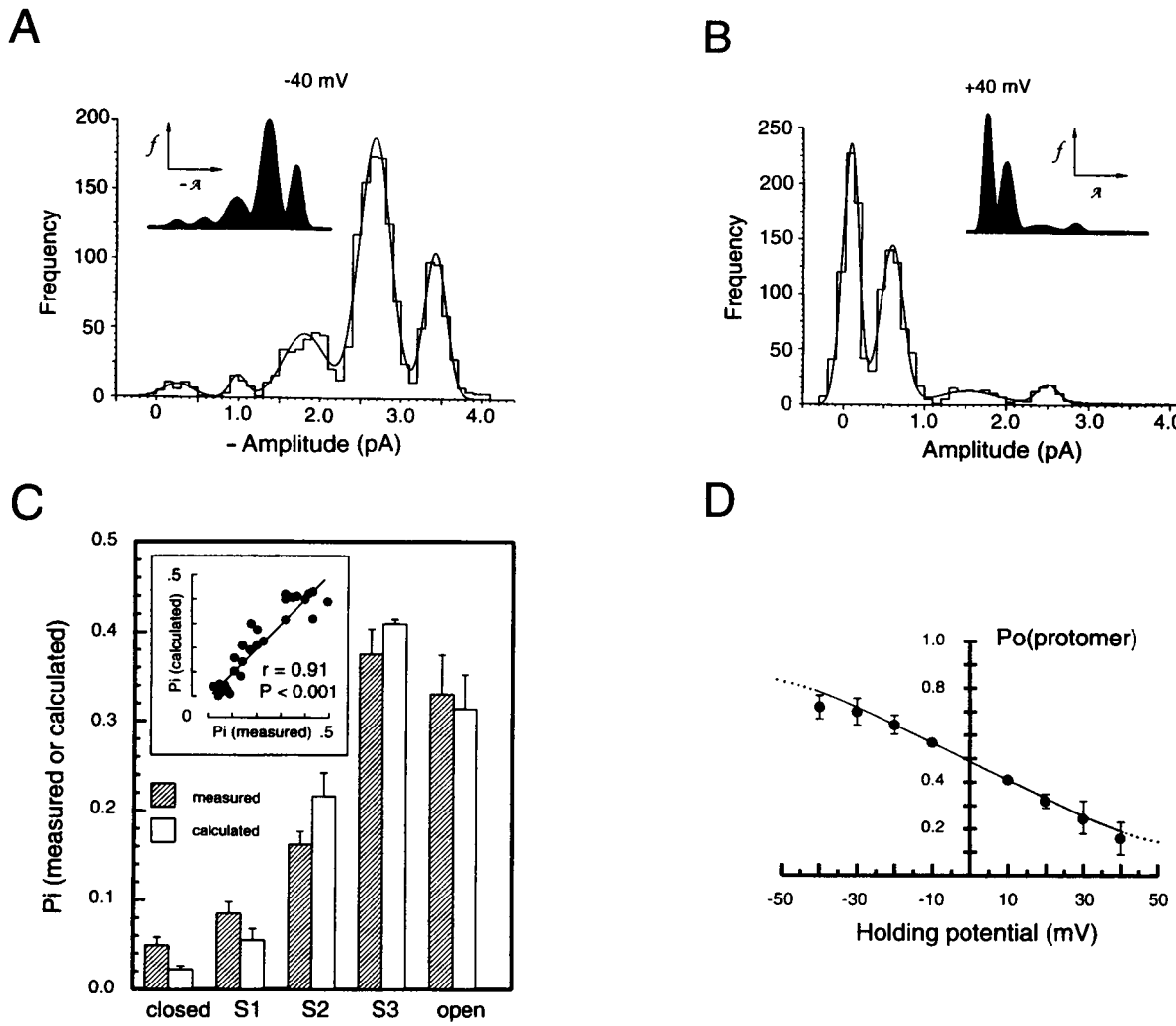

FIGURE 6 Binomial distribution of substate frequencies. (*A* and *B*) Amplitude histograms from 30-s recordings of the same single channel in symmetrical 250 mM choline Cl (data filtered at 0.1 kHz), with least-squares fits to multicomponent Gaussian distributions (continuous lines) to give P_i for each amplitude level. Note that currents were negative at −40 mV, and that very few full openings were detected at +40 mV. Best-fit (maximum-likelihood) P_o(protomer) values for the P_i measurements (see Materials and Methods) were 0.69 at −40 mV and 0.19 at +40 mV. These P_o(protomer) values were used to construct the theoretical binomial distributions inset in both panels (peak variances matched to those of the original data). (*C*) Measured versus predicted residence time at each amplitude level for six channels, recorded under similar ionic conditions at a holding potential of −40 mV (average values, ± SEM, n = 6). P_o(protomer) was 0.73 ± 0.03 (n = 6), and the inset illustrates a highly significant correlation ($p < 0.001$ by t-testing) between the measured and predicted values for P_i (the slope of the line is 0.97). (*D*) The smooth line is a least-squares fit to the Boltzmann equation, with an apparant gating charge of 0.84 and P_o(protomer) = 0.5 at −3.5 mV. Values are averages of at least two independent determinations, ± SEM (n = 4–7 channels) where shown.

plays "multimer"-type substate behavior, and is blocked with relatively low affinity by a range of compounds and ions. Mindful that a minor contaminating membrane fraction could easily contribute highly fusogenic vesicles in bilayer experiments, we recognize that arguments for a particular channel location based solely on the overall purity of a membrane preparation, in the absence of molecular localization or a specific physiological or pharmacological property (e.g., the effect of K^+ channel block on neurosecretory vesicle acidification; Ashley et al., 1994), can be unconvincing. However, we have compelling functional evidence that the novel anion channel described here is present in brain ER, because it is colocalized with brain ER ryanodine-sensitive Ca^{2+} release channels (Ashley, 1989a,b).

The diameter of the channel pore is at least 7 Å, but it has a relatively low single-channel conductance (saturating at 170 pS in choline Cl; Fig. 3 *D*). Calculations after Hille (1984) suggest that a pore this wide should have a conductance approaching 500 pS. With four protochannels, the overall conductance could reach 1–2 nS (similar to VDAC; Colombini, 1994). These data, together with the poor selectivity between anions and cations, suggest that the pore lining or the permeation mechanism may have unusual features. Multiion pore models can be invoked to explain mixed anion and cation permeability in ion channels (e.g.,

TABLE 1 Channel modification

Compound	No. of expts	Conc. used	Type of block	Reversible?	Side of action
9-AC	3	100 μM	Intermediate	Yes	*cis*
DIDS	7	15–100 μM	Complete	No	*cis*
DPC	3	100 μM	No effect	—	—
EA	4	200 μM	Intermediate	ND	ND
Frusemide	2	100 μM	Slow	ND	ND
HEPES	3	10 mM	Slow	ND	ND
IAA-94	14	25–200 μM	Slow/int.	Yes	*cis*
Niflumic acid	2	100 μM	No effect	—	—
NPPB	10	10–100 μM	Int./fast	No	*cis* or *trans*
Puromycin	3	100 μM	No effect	—	—
Zn^{2+}	10	0.5–2 mM	Fast/complete	Yes	*cis*
	9	0.5–2 mM	Complete	Yes	*trans*

"Complete" block means abolition of all channel activity, and "slow," "intermediate" ("int."), and fast block reflect the extent to which individual blocking events could be resolved on the time scale of the recordings (readily, with difficulty, or not at all). See Hille (1994, p. 275). "Inactive" compounds were tested in both chambers. ND, not determined.

Zambrowicz and Colombini, 1993; Franciolini and Nonner, 1994), but the frequent coincorporation of cation channels (permeant, for example, to K^+) prevented detailed tests of such models for the brain ER channel. Nevertheless, the concentration dependence of relative anion versus cation permeabilities supports the idea that the ER channels are multiion pores.

Channel substates and block

Although substates may result from (unobservably) fast changes in channel conformation, including incompletely resolved transitions between open and closed states (Dani and Fox, 1991), they can sometimes be explained by "multimeric" channel complexes with more than one conduction pathway (e.g., Miller, 1982; Matsuda et al., 1989; Morier and Sauve, 1994). The binomial gating behavior of the brain ER anion channel, consistent with independent protomers, strongly supports such an idea. The graded increases we observed in protomer conductance could have resulted from conformational changes induced by the opening of neighboring protomers, or the intercalation of membrane lipids (discussed later). "Multimer"-type substate behavior has also been observed in cardiac mitoplast anion channels (Hayman and Ashley, 1993), although the mitochondrial protomers were functionally coupled in a complex, voltage-dependent manner. The multimer hypothesis was supported by the demonstration that $HEPES^-$ and IAA-94 appeared to interact with individual protochannels, and the voltage dependence of IAA-94 block suggested that the individual protomer blocker-binding sites were located within the membrane electric field. For slow blockers like $HEPES^-$, many more data (collected in recordings lasting longer than the lifetime of most of our bilayers) would be required to measure any voltage dependence, but the fact that HEPES is an impermeant blocker explains why ER anion channels are silent in recording solutions containing Tris/HEPES or Ca-HEPES (Ashley 1989a,b; cf. Smith et al., 1985, 1986).

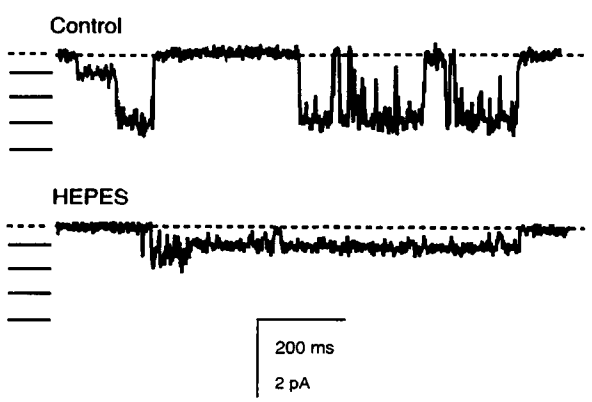

FIGURE 7 Channel block by HEPES. A single channel was exposed to 250 mM choline Cl at a holding potential of −30 mV. The closed state is indicated by a dashed line, and open states by short solid lines placed to the left of the traces (filtered at 0.1 kHz). Note that openings are mainly to substates (especially S3) in the control trace at this holding potential. After 10 mM Tris/HEPES (pH 7.4) is added to both chambers, the channel displays the ~22% substate for long periods, consistent with a "slow" block of one or more protomers.

The kinetics of the ER anion channel can be summarized in terms of the scheme

$$C1 \rightleftharpoons \begin{bmatrix} C2 \rightleftharpoons C3 \rightleftharpoons (C4) \rightleftharpoons O1 \\ C2 \rightleftharpoons C3 \rightleftharpoons (C4) \rightleftharpoons O1 \\ C2 \rightleftharpoons C3 \rightleftharpoons (C4) \rightleftharpoons O1 \\ C2 \rightleftharpoons C3 \rightleftharpoons (C4) \rightleftharpoons O1 \end{bmatrix}$$

where C1 is a relatively long-lived closed or "inactive" state, corresponding to the long interburst closures excluded from the binomial analysis of channel gating, and O1 represents the channel open state (of which there may be more than one), which was not analyzed. C1 closures were too infrequent for detailed lifetime analysis (collecting enough events would require over 30 min of recording time), but they were clearly favored at positive (cytoplasm-ER lumen) potentials. The presence of such a closed state implies there is at least one "master" gate that can shut all four protomers. Bursts of protochannel opening for each of the four inde-

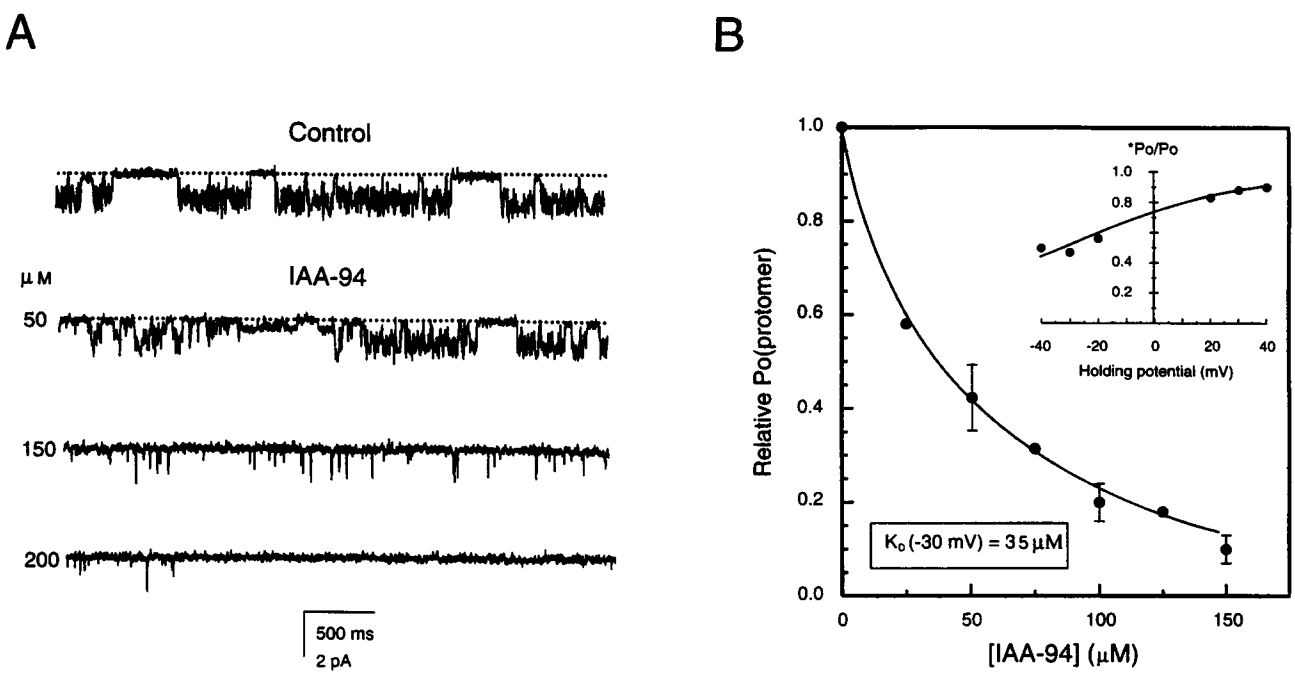

FIGURE 8 Block by IAA-94. (*A*) Selected traces illustrating block by IAA-94 (all recorded at −30 mV, closed states indicated by a *dotted line*, filtered at 0.15 kHz). (*B*) P_o(protomer) values at −30 mV fitted to a single-site inhibition model (*smooth line*, K_D = 35 μM at −30 mV). Each point is the average from at least two independent channels, shown ± SEM for n = 3 measurements. (*Inset*) Voltage dependence of block by 50 μM IAA-94 added to the *cis* chamber (*P_o and P_o represent P_o(protomer) ± drug). The data were fitted as described in the text, giving a K_D(0 mV) value of 135 μM and an effective valence of −0.78.

pendent protochannels correspond to [C2 ⇌ C3 ⇌ (C4) ⇌ O1], where C2 and C3 reflect complicated intraburst behavior, with more closed states than we could adequately resolve, e.g., "(C4)". Runs analysis (Colquhoun and Sakmann, 1985) of highly resolved data to investigate connectivity might relocate some of these closed states outside the square brackets and simplify the interpretation of channel gating behavior.

Bursts of activity often appeared to be delimited by the simultaneous opening or closure of two or more protomers. This was probably an artifact of our limited time resolution. For example, given that the mean lifetime of C3 (the shortest observable intraburst closed lifetime) was 5 ms, the probability of four protochannels opening within that 5 ms was $[1 - \exp(-5/5)]^4 = 0.16$. The value for a recording dead time of 7 ms was twice as high, $[1 - \exp(-7/5)]^4 = 0.32$ (*cf.* Krouse et al., 1986). In this context, superimposed openings of three (or even four) protochannels were not unlikely, especially on exiting C1 at negative holding potentials when P_o(protomer) assumes relatively high values. Some or all of the intraburst transitions were mildly voltage dependent, with a higher protomer P_o at negative compared to positive holding potentials. Summarized in terms of a Boltzmann analysis (Fig. 6 *D*), the protomers had a gating charge of 0.84, and a 0.5 probability of being open at a transmembrane potential of ~0 mV during bursts of channel activity. Although z is very small, it is able to account for the differences in P_o(protomer) at negative and positive potentials. Interestingly, the apex of the bell-shaped relationship between P_o and voltage for an ER cation channel (Schmid et al., 1990; Martin and Ashley, 1993) was centred on 0 mV, although the gating charges were 3–4 times larger. The significance (if any) of these observations awaits the measurement of any ER membrane potential in intact cells.

Channel structure and function

The dimeric structural model of the *Torpedo electroplax* "double-barreled" Cl^- channel (ClC-0) based on single-channel recording (Miller, 1982) has been confirmed by mutagenesis and functional expression (Middleton et al., 1996; Ludewig et al., 1996). Other anion channels may have a similar multimeric arrangement. The block by IAA-94 and HEPES supported the idea that they interacted with individual ER anion channel protomers, but whereas some ClC-type channels now have well-defined roles in cells (Pusch and Jentsch, 1994), the molecular identity and physiological role of the brain ER anion are unknown. The channels do not appear to be protein translocation pores, because they are unaffected by puromycin and they remain active in high-salt conditions (*cf.* Simon and Blobel, 1991). The channel may regulate ER volume or Ca^{2+} release, or be a channel or channel component en route in the secretory pathway to a different cellular destination. Its functional properties may even be further modified post-translation-

ally. The IAA-94-related compound, IAA-23, was used to affinity-purify solubilized Cl^- channels from bovine kidney microsomes (Landry et al., 1987, 1990), including the putative intracellular Cl^- channel p64 (Landry et al., 1992), but the affinity of IAA-94 is probably too low to consider IAA-affinity chromatography to purify the brain ER anion channel.

The anion channel may have a role in intracellular membrane (e.g., ER-*cis* Golgi) trafficking. Although we have no direct evidence for this hypothesis, and we stress that it is highly speculative, several observations are consistent with this idea, given that an intracellular membrane fusion pore might be expected to share some of the characteristics of the fusion pore of secretory and synaptic vesicles (Monck and Fernandez, 1994). For example, recruitment of membrane lipid into an expanding pore complex could explain the increase in protomer conductance as successive protomers open, and bilayer instability at high negative membrane potentials (i.e., at relatively high P_o(protomer) values, extrapolating in Fig. 6 *D* to 1.0 at −100 mV) could reflect irreversible pore expansion preceding membrane fusion.

We are grateful to Rainer Greger for his kind gift of NPPB.

This work was supported by the MRC and by a University of Edinburgh Faculty of Medicine Scholarship to AGC.

REFERENCES

Ashley, R. H. 1989a. Brain microsomes bind ryanodine and contain ryanodine-sensitive calcium channels. *Biochem. Soc. Trans.* 19:254S.

Ashley, R. H. 1989b. Activation and conductance properties of ryanodine-sensitive calcium channels from brain microsomal membranes incorporated into planar lipid bilayers. *J. Membr. Biol.* 111:179–189.

Ashley, R. H., D. M. Brown, D. K. Apps, and J. H. Phillips. 1994. Evidence for a K^+ channel in bovine chromaffin granule membranes: single-channel properties and possible bioenergetic significance. *Eur. Biophys. J.* 23:263–275.

Blatz, A. L. 1991. Properties of single functional chloride channels from rat cerebral cortex neurones. *J. Physiol. (Lond.).* 441:1–21.

Blatz, A. L., and K. L. Magleby. 1985. Single chloride-selective channels active at resting membrane potentials in cultured rat skeletal muscle. *J. Physiol. (Lond.).* 47:119–123.

Chan, T. L., J. W. Greenawalt, and P. L. Pedersen. 1970. Biochemical and ultrastructural properties of a mitochondrial inner membrane fraction deficient in outer membrane and matrix activities. *J. Cell Biol.* 45: 291–305.

Colombini, M. 1994. Anion channels in the mitochondrial outer membrane. *Curr. Top. Membr.* 42:73–101.

Colquhoun, D., and B. Sakmann. 1985. Fast events in single-channel currents activated by acetylcholine and its analogues at the frog muscle end-plate. *J. Physiol. (Lond.).* 369:501–557.

Colquhoun, D., and F. J. Sigworth. 1983. Fitting and statistical analysis of single-channel records. *In* Single-Channel Recording, 1st Ed. B. Sakmann and E. Neher, editors. Plenum, New York. 191–263.

Cotman, C. W. 1974. Isolation of synaptosomal and synaptic plasma membrane fractions. *Methods Enzymol.* 31:445–452.

Dani, J. A., and J. A. Fox. 1991. Examination of subconductance levels from a single ion channel. *J. Theor. Biol.* 153:401–423.

Franciolini, F., and W. Nonner. 1994. A multi-ion permeation mechanism in neuronal background chloride channels. *J. Gen. Physiol.* 104: 725–746.

Gray, E. G., and V. P. Whittaker. 1962. The isolation of nerve-endings from brain: an EM study of cell fragments derived by homogenisation and centrifugation. *J. Anat.* 96:79–87.

Greger, R., E. Schlatter, and H. Gögelein. 1987. Chloride channels in the luminal membrane of the rectal gland of the dogfish (*Squalas acanthias*). Properties of the "larger" conductance channel. *Pflügers Arch.* 409: 114–121.

Hayman, K. A., and R. H. Ashley. 1993. Structural features of a multisubstate cardiac mitoplast anion channel: inferences from single-channel recording. *J. Membr. Biol.* 136:191–197.

Hille, B. 1984. Elementary properties of pores. *In* Ionic Channels of Excitable Membranes, 1st Ed. Sinauer and Associates, Sunderland, MA. 181–204.

Howell, S., R. R. Duncan, and R. H. Ashley. 1996. Identification and characterisation of a homologue of p64 in rat tissues. *FEBS Lett.* 390: 207–210.

Kawano, S., F. Nakamura, T. Tanaka, and M. Hiraoka. 1992. Cardiac sarcoplasmic reticulum chloride channels regulated by protein kinase A. *Circ. Res.* 71:585–589.

Kourie, J. I., D. R. Laver, G. P. Ahern, and A. F. Dulhunty. 1996a. A calcium-activated chloride channel in sarcoplasmic reticulum membranes from rabbit skeletal muscle. *Am. J. Physiol.* 270:C1675–C1686.

Kourie, J. I., D. R. Laver, P. R. Junankar, P. W. Gage, and A. F. Dulhunty. 1996b. Two common types of chloride channel in sarcoplasmic reticulum of rabbit skeletal muscle. *Biophys. J.* 70:202–221.

Krouse, M. E., G. T. Schneider, and P. W. Gage. 1986. A large anion-selective channel has seven conductance levels. *Nature.* 319:58–60.

Lai, F. A., P. H. Erickson, E. Rousseau, Q. Liu, and G. Meissner. 1988. Purification and reconstitution of the calcium release channel from skeletal muscle. *Nature.* 331:315–319.

Landry, D. W., M. A. Akabas, C. Redhead, and Q. Al-Awqati. 1990. Purification and reconstitution of epithelial chloride channels. *Methods Enzymol.* 191:572–582.

Landry, D. W., M. Reitman, E. R. Cragoe, and Q. Al-Awqati. 1987. Epithelial chloride channels: development of inhibitory ligands. *J. Gen. Physiol.* 90:779–798.

Landry, D., S. Sullivan, M. Nicolaides, C. Redhead, A. Edelman, M. Field, Q. Al-Awqati, and J. Edwards. 1992. Molecular cloning and characterisation of p64, a chloride channel protein from kidney microsomes. *J. Biol. Chem.* 268:14948–14955.

Ludewig, U., M. Pusch, and T. J. Jentsch. 1996. Two physically distinct pores in the dimeric ClC-0 chloride channel. *Nature.* 383:340–343.

Martin, C., and R. H. Ashley. 1993. Reconstitution of a voltage-activated calcium-conducting cation channel from brain microsomes. *Cell Calcium.* 14:427–438.

Matsuda, H., H. Matsuura, and A. Noma. 1989. Triple-barrelled structure of inwardly rectifying K^+ channels revealed by Cs^+ and Rb^+ block in guinea-pig heart cells. *J. Physiol. (Lond.).* 413:139–157.

Middleton, R. E., D. J. Pheasant, and C. Miller. 1996. Homodimeric architecture of a ClC-type chloride channel. *Nature.* 383:337–340.

Miller, C. 1982. Open-state substructure of single chloride channels from *Torpedo* electroplax. *Philos. Trans. R. Soc. Lond. Biol.* 299:401–411.

Monck, J. R., and J. M. Fernandez. 1994. The exocytotic fusion pore and neurotransmitter release. *Neuron.* 12:707–716.

Morier, N., and R. Sauvé. 1994. Analysis of a double-barrelled anion channel from rat liver rough endoplasmic reticulum. *Biophys. J.* 67: 590–602.

Palade, P. T., and R. L. Barchi. 1977. On the inhibition of membrane chloride channels by aromatic carboxylic acids. *J. Gen. Physiol.* 69: 879–896.

Pozzan, T., R. Rizzuto, P. Volpe, and J. Meldolesi. 1994. Molecular and cellular physiology of intracellular calcium stores. *Physiol. Rev.* 74: 595–636.

Pusch, M., and T. J. Jentsch. 1994. Molecular physiology of voltage-gated chloride channels. *Physiol. Rev.* 74:813–827.

Rousseau, E., C. Michaud, D. Lefebvre, S. Proteau, and A. Decrouy. 1996. Reconstitution of ionic channels from inner and outer membranes of mammalian cardiac nuclei. *Biophys. J.* 70:703–714.

Rousseau, E., M. Roberson, and G. Meissner. 1988. Properties of single chloride selective channel from sarcoplasmic reticulum. *Eur. Biophys. J.* 16:143–151.

Schmid, A., M. Dehlinger-Kremer, I. Schulz, and H. Gögelein. 1990. Voltage-dependent $InsP_3$-insensitive calcium channels in membranes of pancreatic endoplasmic reticulum vesicles. *Nature.* 346:374–376.

Schmid, A., H. Gögelein, T. P. Kemmer, and I. Schulz. 1988. Anion channels in giant liposomes made of endoplasmic reticulum vesicles from rat exocrine pancreas. *J. Membr. Biol.* 104:275–282.

Simon, S. M., and G. Blobel. 1991. A protein-conducting channel in the endoplasmic reticulum. *Cell.* 65:371–380.

Smith, J. S., R. Coronado, and G. Meissner. 1985. Sarcoplasmic reticulum contains adenine nucleotide-activated calcium channels. *Nature.* 316: 446–449.

Smith, J. S., R. Coronado, and G. Meissner. 1986. Single-channel measurements of the calcium-release channel from skeletal muscle sarcoplasmic reticulum. *J. Gen. Physiol.* 88:573–588.

Sorgato, M. C., and O. Moran. 1993. Channels in mitochondrial membranes: knowns, unknowns and prospects for the future. *Crit. Rev. Biochem. Mol. Biol.* 18:127–171.

Sukhareva, M., J. Morisette, and R. Coronado. 1994. Mechanism of chloride-dependent release of Ca^{2+} in the sarcoplasmic reticulum of rabbit skeletal muscle. *Biophys. J.* 67:751–765.

Tabares, L., M. Mazzanti, and D. E. Clapham. 1991. Chloride channels in the nuclear envelope. *J. Membr. Biol.* 123:49–54.

Tanifuji, M., M. Sokabe, and M. Kasai. 1987. An anion channel of sarcoplasmic reticulum incorporated into planar bilayers: single-channel behavior and conductance properties. *J. Membr. Biol.* 99:103–111.

Townsend, C., and R. L. Rosenberg. 1995. Characterization of a chloride channel reconstituted from cardiac sarcoplasmic reticulum. *J. Membr. Biol.* 147:121–136.

Zambrowicz, E. B., and M. Colombini. 1993. Zero-current potentials in a large membrane channel—a simple theory accounts for complex behaviour. *Biophys. J.* 65:1093–1100.